Lozhechnikova, Alina; Bellanger, Hervé; Michen, Benjamin; Burgert, Ingo; Österberg, Monika

# Surfactant-free carnauba wax dispersion and its use for layer-by-layer assembled protective surface coatings on wood

*Published in:*
Applied Surface Science

*DOI:*
10.1016/j.apsusc.2016.11.132

Published: 28/02/2017

*Document Version*
Peer-reviewed accepted author manuscript, also known as Final accepted manuscript or Post-print

# Surfactant-free carnauba wax dispersion and its use for layer-by-layer assembled protective surface coatings on wood

*Alina Lozhechnikova* [a], *Hervé Bellanger* [b,c], *Benjamin Michen* [b,c], *Ingo Burgert* [b,c], *and Monika Österberg* [a,*]

[a]*Department of Forest Products Technology, School of Chemical Technology, Aalto University, P.O. Box 16300, FI-00076 Aalto, Finland*

[b]*Institute for Building Materials (IfB), Wood Materials Science, ETH Zürich, Stefano-Franscini-Platz 3, 8093 Zürich, Switzerland*

[c]*Applied Wood Materials Laboratory, Empa - Swiss Federal Laboratories for Material Testing and Research, 8600 Dübendorf, Switzerland*

**Corresponding author. Tel.: +358 50 5497218, Email: monika.osterberg@aalto.fi*

## Graphical abstract

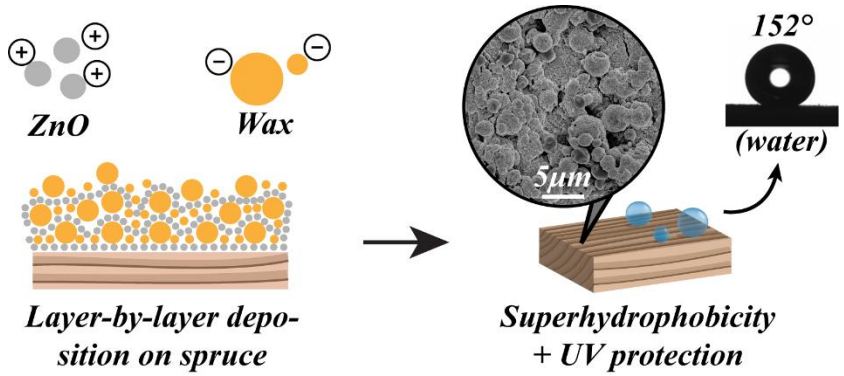

**Abstract**

Protection from liquid water and UV radiation are equally important and a sophisticated approach is needed when developing surface coatings that preserve the natural and well-appreciated aesthetic appearance of wood. In order to prevent degradation and prolong the service life of timber, a protective coating was assembled using carnauba wax particles and zinc oxide nanoparticles via layer-by-layer deposition in water. For this purpose, a facile sonication route was developed to produce aqueous wax dispersion without any surfactants or stabilizers. The suspension was stable above pH 4 due to the electrostatic repulsion between the negatively charged wax particles. The particle size could be controlled by the initial wax concentration with average particle sizes ranging from 260 to 360 nm for 1 and 10 g/L, respectively. The deposition of wax particles onto the surface of spruce wood introduced additional roughness to the wood surface at micro level, while zinc oxide provided nano roughness and UV-absorbing properties. In addition to making wood superhydrophobic, this novel multilayer coating enhanced the natural moisture buffering capability of spruce. Moreover, wood surfaces prepared in this fashion showed a significant but not extensive reduction in color change after exposure to UV light. A degradation of the wax through photocatalytic activity of the ZnO particles was measured by FTIR, indicating that further studies are required to achieve long-term stability. Nevertheless, the developed coating showed a unique combination of superhydrophobicity and excellent moisture buffering ability and some UV protection, all achieved using an environmentally friendly coating process, which is beneficial to retain the natural appearance of wood and improve indoor air quality and comfort.

**Keywords:** Wood modification, carnauba wax, ZnO, hydrophobicity, UV resistance, moisture buffering

## 1. Introduction

Wood is an exceptionally versatile material that has been used in house, furniture and boat construction for millennia. Its mechanical strength, visual appearance, thermal insulation and humidity-buffering properties make it a unique material for humankind. As the demand for green, renewable and sustainable materials keeps growing in modern societies, wood is gaining popularity again. Raising environmental concerns has increased the interest for wood as an alternative to concrete, gypsum boards and fossil-based synthetic materials. Additionally, some studies suggest that the moisture-buffering ability of wood used indoors has the potential to reduce the amplitude of fluctuations in relative humidity and thus, reduce the energy demand for HVAC (heating, ventilation, and air conditioning) systems in buildings [1-3]. However, while the appearance and tactility of wood are often perceived superior to that of synthetic materials, its hydrophilic nature creates a number of practical problems that affect its service life. In direct contact with water, some of the arising issues are dimensional instability, including deformation, twisting and cracking, and the creation of favorable conditions for fungal growth with subsequent degradation. Changes in color and chemical composition of wood surfaces exposed to UV light is another issue that should be overcome. Sensitivity of timber is mostly attributed to lignin degradation into small molecular weight compounds and their further removal from cell wall by combined interactions with water; this in turn increases hydrophilicity of the surface and promotes fungal growth [4].

To tackle these problems, a large body of research is available on wood surface modification [5]. Common hydrophobization methods include grafting of silicone and fluorine-containing compounds, deposition of metal oxide nanoparticles and impregnation with various chemicals [6]. Many of these techniques are very effective in hydrophobizing wood and even achieve omniphobic

61 surface properties [7], though they generally overlook the effect of the treatment on the humidity-
62 buffering properties at the surface as well as possible toxicity and the environmental impact of the
63 utilized compounds and processes. When it comes to protection from UV degradation,
64 modifications with ZnO and $TiO_2$ particles, treatments with ionic liquids and grafting of UV
65 stabilizers are commonly used [8-11]. Protection from water and UV light are equally important
66 and call for novel approaches and the development of sustainable treatments that prevent
67 photodegradation, protect from water but do not decrease moisture buffering ability of wood. For
68 instance, by combining hydrophobic and UV absorbing components within one coating system.
69 An easy and environmentally friendly way that would allow a controlled deposition of various
70 functional materials on the surface is the layer-by-layer (LbL) deposition. A method of building
71 up thin multilayers of oppositely charged colloidal particles was discovered already in 1966 [12],
72 but it has been rarely applied to wood or wood-derived materials: polyelectrolyte multilayers,
73 using synthetic polymers, were successfully used to modify surface properties of cellulose fibers
74 [13] and wooden surfaces, in an attempt for better control of the surface chemistry [14].
75 Combination of polyelectrolyte multilayers and colloidal wax particles was also shown to reduce
76 sensitivity of cellulose fibers towards water [15]. Recently, a combination of polyelectrolytes and
77 titanium dioxide layers resulted in a superhydrophilic wooden surface, which, after modification
78 with stearic acid, turned into a hydrophobic one. In addition, the $TiO_2$ particles in this coating
79 functioned as UV light absorber and reduced discoloration following UV exposure [16].

80 Wax emulsions have been used in commercial water-repellent products for years [17,18].
81 Additionally, it was previously reported that high loadings of waxes can slow down
82 photodegradation, by reducing moisture content of the wood and partly absorbing the UV
83 light[19]. Therefore, natural waxes could be an interesting alternative to synthetic polymers when

protecting wooden surfaces [20]. Carnauba wax is among the hardest natural waxes and is composed primarily of C24 and C28 esters, C32 and C34 straight-chained primary alcohols, and hydroxy-fatty acids [21,22]. Due to its high melting point of 83-86ºC, it is extensively used as an additive in polishes for cars, leather and floors, glazing for paper, foods and pharmaceuticals, as well as drug delivery [23]. The most common ways to produce carnauba wax dispersions are rotor-stator homogenization [24], high-pressure homogenization [25], and ultrasonication [26], usually combined with various surfactants. As an alternative to using surfactants, a carnauba wax emulsion was also successfully obtained by self-emulsification in organic alcohols [27]. However, addition of the surfactants to the wax dispersion might affect the surface energy of the particles and reduce their hydrophobicity in further applications, while organic solvents are less environmentally friendly than water-borne systems.

Herein, we propose a new and facile method to produce a stable aqueous dispersion of carnauba wax micro- and nanoparticles. To the best of our knowledge, this is the first work where such an aqueous dispersion was prepared without addition of surfactants or emulsifiers. The anionic wax particles are used in combination with commercial cationic ZnO nanoparticles to obtain a protective wood coating via water-based LbL route. The ZnO nanoparticles were selected due to their UV absorbing properties as well as their small size, which enables the generation of nanoscale roughness indispensable for the fabrication of superhydrophobic surfaces. Moreover, the ZnO nanoparticles can be used at neutral pH, unlike commonly used $TiO_2$ particles that require significant pH adjustments in order provide a stable nanodispersion [28]. Additionally, ZnO nanoparticles are known to exhibit antifungal [29,30] and antibacterial [31,32] properties, which were not investigated in current work, but are generally of interest in wood modification.

## 2. Experimental

### *2.1. Materials*

Carnauba wax (CAS 8015-86-9) and Zinc oxide (ZnO) nanoparticle dispersion (<35nm average particle size, 50 wt.% in $H_2O$, CAS 1314-13-2) were purchased from Sigma-Aldrich. Norway spruce (*Picea abies*) samples of typically 5 cm × 5 cm × 0.6 cm in radial × longitudinal × tangential direction, respectively, were used for coatings. For moisture buffering experiments samples of 3 cm × 3 cm × 1 cm were coated.

### *2.2. Preparation and Characterization of Wax Dispersion*

The dispersion of wax particles was produced by combining different ratios of distilled water and carnauba wax. This mixture was heated up on a hot plate until 90ºC temperature was reached and then sonicated for 5 minutes using Ultrasonic Probe Sonifier S-450 with 1/2" extension (Branson Ultrasonics). The final dispersion was then cooled in an ice bath and filtered through a filter funnel with 40-100 µm nominal maximal pore size.

The electrophoretic mobility and average particle size were measured using Zetasizer Nano-ZS90 (Malvern Instrument Ltd., Worcestershire, U.K.). All measurements were conducted at a wax concentration of 1 g/L. Dynamic Light Scattering (DLS) size measurements of the wax dispersion prepared at 1 g/L were performed on the day the dispersion was prepared, then after 7 days and after 3 months to monitor colloidal stability. Size measurements were repeated on two samples with at least 5 measurements per sample. The Z-average and the polydispersity index (PDI) of all measurements was calculated by the operating software. For electrophoretic mobility measurements, the pH of the wax dispersion was adjusted with dilute HCl and NaOH solutions. The ζ-potential was calculated from the electrophoretic mobility data by the instrument software using the Smoluchowski model. Atomic force microscopy (AFM) imaging in air was used as a

complementary method to estimate the size of wax particles dried on a mica surface. For this purpose, a NanoscopeV MultiMode scanning probe microscope (Bruker Corporation, Massachusetts, USA) in tapping mode was used. Silicon cantilevers (NSC15/AIBS, MicroMasch, Tallinn, Estonia) with driving frequencies around 300–360 kHz and the radius of the tip less than 10 nm (according to the manufacturer) were used for imaging. Images of the surface were taken in at least three different places.

### *2.3. Layer-by-Layer (LbL) Assembled Coatings*

ZnO was selected as a cationic component of this LbL system. The isoelectric point of the zinc oxide in water is pH 9.5, and below this pH the particles have an overall positive charge [33]. Wood surface in aqueous solution, on the other hand, is rich in hydroxyl groups and has an anionic character [14,16]. The surface of the wax particles is also negatively charged, as will be discussed in subsection 3.1 of this article. Before coating, the pH of the zinc oxide dispersion was adjusted to pH 6.8-6.9 with dilute HCl, in order to match the pH of the wax dispersion. Multilayer coatings were applied onto the radial surface of water saturated Norway spruce samples through consecutive deposition of zinc oxide and wax particles. Zinc oxide was always deposited as a first layer and the coating process was always finished with wax as a last layer. The samples were immersed into particle dispersions for 30 minutes during formation of first bilayer and for 5 minutes for all consecutive bilayers, and then rinsed for 15 minutes in three different beakers with deionized water to remove particle excess. When the desired number of bilayers was assembled, wooden samples were dried in oven for 1 hour at 65ºC, and then left at ambient conditions overnight. In order to study the influence of wax concentration on the formation of the coating, 1 and 10 g/L wax dispersions were used for the layer-by-layer assembly, while the concentration of ZnO was kept constant at 10 g/L.

Some of the coated samples were further annealed in oven at 70, 80, 90, 100 or 110ºC for 30 minutes to investigate the effect of wax melting on coating properties.

*2.4. Characterization of LbL coated wooden surfaces*

The static contact angle of water (CA) was measured using a contact angle meter CAM 200 (KSV Instruments Ltd., Helsinki, Finland). 7 $\mu$L water droplets were dispensed on wooden surfaces and after one minute images were taken by a built-in digital camera. The longer contact time (one minute) was chosen to emphasize the good performance of the coating over time, when in contact with water. The images were then analyzed and the full Young-Laplace equation was used to determine the contact angle from the shape of the drop. For every type of coating two samples were tested and CA was determined on at least three positions on each sample. Prior to CA measurements wood samples were conditioned at 50% RH and 23ºC for at least two weeks. For the sliding angle experiments, drops were deposited on the surface and samples were then slowly tilted until drops rolled off the surface. Last image taken just before the drop slided off the surface was used for sliding angle calculations.

Topography maps of 560×420 $\mu$m area were obtained with a 3D Optical Microscope ContourGT-K 3D (Bruker Corporation, Massachusetts, USA) on three random spots on each sample. Vision64 onboard software was then employed to analyze the data and to calculate the average roughness $S_a$.

Scanning electron microscopy (SEM) was carried out using a FEI Nova NanoSEM 230 instrument (FEI, Hillsboro, Oregon, USA) at an accelerating voltage of 5 kV and a working distance of 5 mm. Wood samples were placed on a specimen holder and coated with a platinum layer of

approximately 7 nm by sputtering at $5 \times 10^{-2}$ mbar; Argon was used as gas carrier (BAL-TEC MED 020 Modular High Vacuum Coating Systems, BAL-TEC AG, Liechtenstein).

The moisture buffering measurements were performed in accordance with the NORDTEST method [34]. The wood samples were sealed with aluminum adhesive tape on all but one radial surface, conditioned at 50% RH and 23ºC until their weight was stable and then placed into climatic test chamber (Rumed 4201, Rubarth, Apparate GmbH, Germany). Inside the chamber, the radial surface of the samples was exposed to cycles of high (75% for 8 h) and low (33% for 16 h) levels of relative humidity. During these cycles, masses of the samples were monitored with a New Classic MS 204S balance with a precision of 0.01 mg (Mettler Toledo, Switzerland). Weight gains and weight losses were recorded for each sample during 72 h of exposure to humidity changes and the average value between gain and loss was taken ($\Delta m$). By normalizing this value by the open surface area ($S$) of the sample and the change in relative humidity ($\Delta RH$), the Moisture Buffer Value (MBV) was calculated, according to following equation:

$$MBV_{practical} = \frac{\Delta m}{S \times \Delta RH} \quad (1)$$

For each treatment, three parallel samples were tested. More detailed information about moisture buffering and NORDTEST experimental procedures can be found elsewhere [20,34].

UV-Vis reflectance spectra were acquired with a lambda 650 UV spectrometer (Perkin Elmer) equipped with a 150 mm integrating sphere in the range of 190 nm to 800 nm. The spectra of untreated wood were acquired at three different spots (approximatively 15 mm length and 10 mm width), perpendicularly to the fibers direction in order to measure latewood and earlywood. Measurements were performed in total reflectance mode, i.e. specular and diffuse reflectance were collected. From the UV-Vis spectra, the L*, a*, b* parameters (CIELAB) and general color change

ΔE were calculated to quantify color changes. The illuminant was D65, which simulates noon daylight, and the observer was set at 2°. Thereby, $L^*$ represents lightness (black to white), while a* and b* are the chromaticity coordinates (representing red to green, and yellow to blue, respectively). The following equation was used to calculate $\Delta E$ from $L^*$, $a^*$ and $b^*$ values[35]:

$$\Delta E = [(\Delta L^*)^2 + (\Delta a^*)^2 + (\Delta b^*)^2]^{1/2} \quad (2)$$

Treated samples were exposed to UV radiation in a UV chamber of type UVA Cube 400 (Honle UV America, Inc.) equipped with a Sol500 lamp for 10 days in total. Under radiation the temperature in the UV chamber was around 40 °C

The FTIR (Fourier Transform Infrared Spectroscopy) spectroscope used was a Tensor 27 (Bruker Corporation, Massachusetts, USA) equipped with an ATR (Attenuated Total Reflectance). Measurements were done with 32 scans and a resolution of 4 $cm^{-1}$. All spectra were normalized to a wood specific peak at 1030 $cm^{-1}$, which originates mostly from C–O stretching of secondary alcohols in cellulose [36]. This peak is not affected by the wax nor the ZnO.

## 3. Results and Discussion

### *3.1. Wax dispersion*

A dispersion of carnauba wax particles with a concentration of 1 g/L was produced from pure wax and water with no additional emulsifiers or stabilizers. The initial pH of the dispersion was in the neutral range (pH=6.8-6.9) at which a ζ-potential of -53±0.4 mV was measured. This net negative surface charge of wax particles provided electrostatic double-layer repulsion and stabilized the dispersion [37]. The origin of these electrostatic charges can be understood by the presence of hydrophilic and functional groups, such as –OH, –COOH, –CHO, in natural waxes [38]. When

melted wax is being dispersed in water, these hydrophilic groups can rearrange toward the polar water phase, thus, leaving the particle interface more hydrophilic than its core. This hypothesis correlates well with the findings of Bayer *et al*, who found that heat treatment of a carnauba wax film resulted in rearrangement of its hydrophilic groups toward a hydrophilic glass substrate [27]. As presented in Figure 1a, the absolute value of the ζ-potential decreased with lower pH values, but the dispersion remained stable at pH>4. At pH<4 the suspension flocculated rapidly, indicating that the lower surface charge at this pH is not sufficient for electrostatic stabilization.

The stability of the wax dispersion at neutral pH was further confirmed by DLS measurements over time. The size distributions measured after one day, one week and three months are shown in Figure 1b. The intensity distribution is nearly the same on the day the dispersion was produced and after 3 months of storage time. Analysis of particle size and polydispersity index (PDI) resulted in Z-average values of 261±4 nm (PDI=0.22) and 250±5 nm (PDI=0.23) measured after 1 day and 3 months, respectively. In order to confirm the size of particles and gain insight into their morphology, a drop of wax suspension was dried on a freshly cleaved mica sheet and imaged with AFM. Height and phase images, shown in Figure 1c and 1d, respectively, indicate a spheroidal geometry of wax particles. Further, AFM images confirm the polydispersity of the suspension characterized by light scattering; the largest primary particles seen on the image are around 350 nm while the smallest ones are in the range of 50-60 nm. However, a quantitative size analysis of the AFM images is challenging due to the formation of agglomerates during drying. These drying artifacts make it difficult to assess the dispersion state by microscopic techniques [39]. Moreover, the particle size can be controlled by the wax concentration during the preparation of the suspension. The average size of wax particles increased with increasing wax concentration for 1, 5 and 10 g/L as shown in Table 1. Z-average values between 260 and 360 nm were measured for

wax concentrations between 1 and 10 g/L. Note that for the deposition of wax particles via the LbL approach, only dispersions of 1 and 10 g/L were used; their characterization by DLS is summarized as well in Table 1.

**Table 1.** Wax dispersions characterized by dynamic light scattering. *t**: time after preparation of suspension, PDI: Polydispersity index

| Wax concentration g/L | t* | Z-average nm | PDI |
|---|---|---|---|
| 1 | 1 day | 261±4 | 0.22 |
| 1 | 1 week | 253±5 | 0.21 |
| 1 | 3 months | 250±5 | 0.23 |
| 5 | 1 day | 318±4 | 0.27 |
| 10 | 1 day | 362±9 | 0.27 |

*3.2. Buildup of multilayer coatings*

Multilayer coatings consisting of zinc oxide and carnauba wax particles were assembled on wooden surfaces. The presence of wax and ZnO on spruce was verified using FTIR spectroscopy after LbL deposition of particles in suspensions with a concentration of 10 g/L. Figure 2a shows the FTIR spectra of untreated wood (black curve) and wood coated with 8 bilayers of wax and zinc oxide (blue curve). After modification, an intense peak at 405 $cm^{-1}$ shows the presence of ZnO nanoparticles. The Carnauba wax can be identified by the main spectral features of esters with a carbonyl (C=O) stretching at 1735 $cm^{-1}$ and C-C(=O)-O stretching at 1165 $cm^{-1}$, as well as by the methylene vibration at 2916 $cm^{-1}$ and 2848 $cm^{-1}$ (stretching), 1472 $cm^{-1}$ and 1463 $cm^{-1}$ (scissoring), 729 $cm^{-1}$ and 719 $cm^{-1}$ (rocking) [36]. In addition, the peak at 1604 $cm^{-1}$ shows the presence of carboxylate and confirms the origin of the negative surface charge of the particles discussed before.

The resulting coating is almost transparent as shown by reflectance spectra in Figure 2b: The difference between coated and uncoated wood in the visible range (from 400 to 800 nm) is negligible with a total color change of $\Delta E=1.95\pm0.24$. However, the reflectance of the coated sample in the UV range (from 190 to 380 nm) is significantly decreased indicating UV absorption facilitated by ZnO nanoparticles. Moreover, in the range from 240 to 320 nm the spectrum becomes flat indicating that the coating shields the peak at 280 nm belonging to lignin [40], which is known to be the most UV-sensitive wood compound and mainly responsible for UV-induced color changes [41]. The protective effect of the coating on the color change during UV exposure will be discussed later.

### *3.3. Effect of processing parameters on the wettability and morphology of the multilayer coatings*

The morphology of the multilayer coating was analyzed by SEM in Figure 3. Images were taken on unmodified spruce (Figure 3a) and spruce coated with 8 bilayers of ZnO/wax at different wax concentrations (Figure 3b and 3c). The underlying micro structure of wood was mostly preserved regardless of the wax concentration and particle deposition resulted in relatively thin coatings, which did not significantly affect the natural appearance of wood. While the concentration of the ZnO dispersion was kept constant at 10 g/L during the LbL deposition, the effect of the wax concentration on the coating morphology was investigated for 1 g/L and 10 g/L. Coatings prepared at lower wax concentration showed less wax particles on the wood surface (Figure 3b and 3c) indicating a strong impact of the particle suspension concentration on the surface coverage during the LbL process. The wood surface as well as immobilized wax particles were densely coated with ZnO particles, which introduced a nanoscale roughness as seen in the high magnification micrographs (Figure 3 b3 and c3). The coating was terminated by a last deposition of wax particles that did not have any ZnO particles adsorbed onto their surface and, therefore, displaying a smooth

interface. In Figure 3 c3, the presence of both, wax particles coated and not coated with ZnO indicated by white and green arrow, respectively, is shown and pointing out a low surface coverage by the last wax layer.

When it comes to designing highly hydrophobic and superhydrophobic surfaces, two parameters are of special importance: surface energy and complex surface roughness [42]. Wood surfaces already have a micron sized (anisotropic) roughness (see Figure 3a1 and Table 2). In this work, wax particles increased the roughness at the sub-micron scale (Figure 3 and Table 2) and provided a low surface energy, whereas zinc oxide provided additional nano-scaled roughness. The effect of different multilayer coatings on the contact angle (CA) of water was studied as a measure of their hydrophobicity. Figure 4 shows CA values for unmodified spruce and samples coated with 1 or 8 bilayers of ZnO and wax. Concentration of the ZnO dispersion was always 10 g/L, while wax concentration was 1 or 10 g/L.

As shown in Figure 4, the wooden surfaces turned highly hydrophobic already after 1 bilayer of coating, with CA reaching 145-147º regardless of the wax concentration. However, as the amount of layers increased, the influence of wax concentration increased as well, resulting in a slightly smaller CA of 135º for 1 g/L wax and an even higher CA of 155º for surfaces where 10 g/L wax was used, respectively. One explanation for this result could be that when a lower wax concentration is used, less wax particles are deposited per layer and their average size is smaller, therefore the ratio of ZnO/wax in this coating is increased compared to the coating deposited at higher (10 g/L) wax concentration. In this way, after 8 bilayers, the contribution from the hydrophilic nature of zinc oxide starts to dominate over the contribution from the nano-roughness it provides, resulting in a smaller CA. Topography SEM images of coated wood in Figure 3 also support this assumption. When wax in 10 g/L concentration was used (Figure 3 c1- c3), there are

much more visible wax particles on the surface and the roughening of the surface was more substantial in comparison to when 1 g/L dispersion was used (Figure 3 b1-b3). However, it must be noted that these variations in CA are small compared to the large difference between coated and uncoated wood.

Wooden surfaces coated with 8 bilayers of 10 g/L dispersions can be described as superhydrophobic, as static water contact angle reached more than 150° [43,44]. Video showing wetting of the coated wood surface with 8 bilayers of ZnO/wax is available and accompanies the electronic version of this manuscript. Sliding angle experiments were performed on this surface in order to determine if the interface is in the Wenzel or Cassie-Baxter state. It was found that small drops (7 $\mu$L) do not roll off the surface and stay attached to it even when surface is tilted to 90° angle or turned upside down. These findings suggest that the interface might be in "Cassie impregnating" wetting state, similar to that one of rose petals [45]. However, when bigger drops (13 $\mu$L) were deposited on the surface, sliding angle was found to be 23.6±4.9°(note, that the anisotropy of the wood surface did not significantly influence the roll-off angle as water drops behaved similar regardless of the tilting axis). This indicates a wetting transition usually attributed to a decrease in Laplace pressure [46]. Once the balance between the surface tension and the weight of the drop is reached, the drop will roll off the surface. This transitional state between Wenzel and Cassie-Baxter regimes is characterized by partial wetting of the surface with water, in contrast to Cassie "Lotus leaf" state, where air pockets prevent liquid from wetting the surface [43].

### *3.4. Effect of thermal annealing on wetting*

Thermal treatment might enhance the mobility of wax molecules, causing a shift in crystallinity and rearrangement of various aliphatic and aromatic esters in different directions [27], thus,

changing the surface energy. Differential scanning calorimetry thermograms of pure carnauba wax reveal that softening of the wax starts already at 50-60°C [47], but in this work all wood samples were dried at 65°C after the coating process. Therefore, the effect of thermal treatment on water CA was investigated in 65-110°C range. Samples were coated with 8 bilayers of 10 g/L ZnO/wax particles and then annealed in an oven for 30 minutes at different temperatures. During the heat treatment, topography of the samples changed noticeably (Figure 5a and 5b), despite rather minor changes in hydrophobicity (Figure 5c). The roughness of the coated samples (Table 2) was not significantly affected by thermal treatment up to 100°C. However, after treatment at 110°C it decreased noticeably which might be due to the melting of the wax particles and the partial film-formation on the surface. However, the fact that the roughness is decreasing while the CA tends to increase with temperature, may confirm the hypothesis that the surface energy is changed by the heat treatment.

**Table 2.** Average roughness of uncoated and coated wood surfaces (with 10 g/L of wax and ZnO dispersions) after different heat treatments

| Samples | Heat treatment, °C | Average roughness $S_a$, µm | Standard deviation |
|---|---|---|---|
| Spruce | none | 4.5 | 0.9 |
| 1 bilayer | 65 | 5.0 | 1.7 |
| 8 bilayers | 65 | 8.0 | 1.2 |
| 8 bilayers | 70 | 7.9 | 1.0 |
| 8 bilayers | 80 | 7.8 | 1.2 |
| 8 bilayers | 90 | 7.8 | 0.8 |
| 8 bilayers | 100 | 7.9 | 0.9 |
| 8 bilayers | 110 | 5.0 | 0.9 |

Figure 5a shows SEM images of coated samples annealed at various temperatures. The most significant changes on the surface occurred between 90ºC and 110ºC (the melting temperature of wax ≈83-86ºC)as can be seen on close-up SEM images in Figure 5b. It appears that wax particles are melting and forming a film on the surface with zinc oxide particles being partly submerged into the wax matrix rather than being on its surface. Considering that carnauba wax is a relatively hard matrix, it might protect the ZnO component and prevent it from leaching from the surface, thus possibly making the coated surface more durable.

### *3.5. Moisture buffering*

Wood samples coated with 10 g/L ZnO and wax particles were exposed to changes in relative humidity, simulating daily humidity changes in a living space. Their moisture buffering performance was then evaluated by monitoring the moisture uptake and release. As can be seen from Figure 6, coating not only preserved moisture buffering ability of natural timber, but actually enhanced it. MBV increased from 1.12 for unmodified spruce to 1.46-1.41 for coated and 1.35 for coated and annealed surface, therefore, all surfaces have “good” level of moisture buffering according to NORDTEST classification [34]. Similar results were observed in our previous work, where addition of wax particles alone increased the MBV of the surface [20]. It is possible that the hydrophilic nature of zinc oxide particles is responsible for the improved moisture buffering performance, as water can adsorb on the surface of ZnO particles. Additionally, higher roughness, and thus an increased specific surface area of the coated samples, may provide adsorption sites for moisture and increase the MBV. Another reason for the enhanced water vapor uptake may be the leaching of the extractives during LbL process and consequently higher hygroscopicity of wood.

In summary, ZnO/wax coating of the wooden surface provided superhydrophobicity and enhanced moisture-buffering performance, which is a great combination. Superhydrophobic surfaces are easy to clean and care for, while good moisture buffering helps to even out the fluctuations and reduces excessive levels of humidity in the air.

### *3.6. Effect of LbL coating on UV degradation*

The coated wood samples were exposed to UV irradiation and their color change was monitored over time. The protective effect of the coating can be seen in Figure 7, which shows photographs of the coated and uncoated wood before and after the UV exposure. The total color change, $\Delta E$, of coated and control samples was recorded as a function of the UV exposure time in Figure 8. After 10 days of exposure the untreated spruce showed a $\Delta E$=17.6±0.3, while the total color changes were 10.6±0.3 and 11.6±0.5 for the coated and annealed sample, respectively.

Wood samples were analyzed by FTIR during the UV exposure experiment as shown in Figure 9. The intensity of the wax specific peaks decreased with the exposure time and vanished almost completely after 10 days of UV irradiation indicating the degradation of the wax particles. This is attributed to photocatalytic degradation of the wax by the ZnO nanoparticles. Similar changes have been observed on a clear coating of ZnO embedded in a polymer matrix [8]. Two new peaks at 1642 $cm^{-1}$ and 1590 $cm^{-1}$ appeared (Figure 9; dashed black line), which could be attributed to $CO_2$ adsorption on ZnO interface [48]. This increasing $CO_2$ adsorption can be explained by an increased accessible ZnO surface, which is available after the degradation of wax previously in contact with ZnO. Moreover, the disappearance of the characteristic lignin peak at 1510 $cm^{-1}$ (Figure 9; dashed red line) with UV exposure time showed that the protection effect is limited. In conclusion, the protective effect against UV light was proven, however, more layers would be needed to provide

382 a superior and sufficient shielding of UV light and additives such as HALS (Hindered Amine Light
383 Stabilizers) should be added to the raw wax in order to protect it against the photocatalytic
384 degradation due to the interfacial contact with ZnO nanoparticles.

385 **4. Conclusions**

386 An aqueous carnauba wax dispersion was prepared by ultrasonication in water from pure wax,
387 without any additional surfactants or stabilizers. The method mainly yields particle sizes in the
388 sub-micron range and provides stable wax suspensions of up to 10 g/L even after three months of
389 storage. The negatively charged wax colloids were combined with positively charged ZnO
390 nanoparticles for a protective surface coating on wood assembled via simple and environmentally
391 friendly layer-by-layer process. Wax particles enhanced the natural roughness of wood on the
392 micro scale, while zinc oxide provided nano-roughening. This combination resulted in a
393 hydrophobization of the wood surface. An interesting addition to the superhydrophobicity of the
394 surface is its retained moisture buffering properties. Additional thermal treatment of the coated
395 wood slightly increased hydrophobicity by altering surface energy of wax particles and
396 presumably improved coating stability. The presence of zinc oxide in the multilayer coating
397 reduced the total color change of the wood surface during UV irradiation. However, wax particles
398 were degraded during irradiation. To improve the UV protective effect of the coating and protect
399 the wax phase from the photocatalytic degradation, additional additives, like free radical
400 scavengers or HALS would be needed.

401 This paper presents a proof of concept that LbL is an efficient technique to modify wood surfaces
402 using charged particles. The developed process is water-based and very simple; it does not require
403 harmful solvents or harsh conditions. The method is not restricted to ZnO particles, other positively

charged components could be tested in order to make the final product even more environmentally friendly.

**Acknowledgements**

Aalto Energy Efficiency Research Programme is acknowledged for funding through the WoodLife Project. Anja Huch and Esther Strub are acknowledged for help with SEM imaging.

**References**

[1] M. Woloszyn, T. Kalamees, M. Olivier Abadie, M. Steeman, A. Sasic Kalagasidis, The effect of combining a relative-humidity-sensitive ventilation system with the moisture-buffering capacity of materials on indoor climate and energy efficiency of buildings, Build. Environ. 44 (2009) 515-524. doi:http://dx.doi.org/10.1016/j.buildenv.2008.04.017.

[2] O.F. Osanyintola, C.J. Simonson, Moisture buffering capacity of hygroscopic building materials: Experimental facilities and energy impact, Energy Build. 38 (2006) 1270-1282.

[3] S. Hameury, Moisture buffering capacity of heavy timber structures directly exposed to an indoor climate: a numerical study, Build. Environ. 40 (2005) 1400-1412. doi:http://dx.doi.org/10.1016/j.buildenv.2004.10.017.

[4] C.A.S. Hill, Wood modification: Chemical, Thermal and Other Processes, (2006) 239.

[5] M. Petrič, Surface Modification of Wood, Reviews of Adhesion and Adhesives. 1 (2013) 216-247. doi:10.7569/RAA.2013.097308.

[6] C. Wang, C. Piao, From Hydrophilicity to Hydrophobicity: A Critical Review - Part II: Hydrophobic Conversion, Wood Fiber Sci. 43 (2011) 41-56.

[7] H. Guo, P. Fuchs, K. Casdorff, B. Michen, M. Chanana, H. Hagendorfer, Y.E. Romanyuk, I. Burgert, Bio-Inspired Superhydrophobic and Omniphobic Wood Surfaces, Adv. Mater. Interfaces. (2016) 1600289. doi:10.1002/admi.201600289.

[8] J. Salla, K.K. Pandey, K. Srinivas, Improvement of UV resistance of wood surfaces by using ZnO nanoparticles, Polym. Degrad. Stab. 97 (2012) 592-596. doi:http://dx.doi.org/10.1016/j.polymdegradstab.2012.01.013.

[9] Q. Sun, Y. Lu, H. Zhang, H. Zhao, H. Yu, J. Xu, Y. Fu, D. Yang, Y. Liu, Hydrothermal fabrication of rutile TiO2 submicrospheres on wood surface: An efficient method to prepare UV-protective wood, Mater. Chem. Phys. 133 (2012) 253-258. doi:http://dx.doi.org/10.1016/j.matchemphys.2012.01.018.

[10] S. Patachia, C. Croitoru, C. Friedrich, Effect of UV exposure on the surface chemistry of wood veneers treated with ionic liquids, Appl. Surf. Sci. 258 (2012) 6723-6729. doi:http://dx.doi.org/10.1016/j.apsusc.2011.12.050.

[11] H. Guo, P. Fuchs, E. Cabane, B. Michen, H. Hagendorfer, Y.E. Romanyuk, I. Burgert, UV-protection of wood surfaces by controlled morphology fine-tuning of ZnO nanostructures, Holzforschung. 70 (2016) 699-708. doi:10.1515/hf-2015-0185.

[12] R.K. Iler, Multilayers of colloidal particles, J. Colloid Interface Sci. 21 (1966) 569-594. doi:http://dx.doi.org/10.1016/0095-8522(66)90018-3.

[13] L. Wågberg, S. Forsberg, A. Johansson, P. Juntti, Engineering of fibre surface properties by application of the polyelectrolyte multilayer concept. Part I: Modification of paper strength, J Pulp Pap Sci. 28 (2002) 222-228.

[14] S. Renneckar, Y. Zhou, Nanoscale coatings on wood: Polyelectrolyte adsorption and layer-by-layer assembled film formation, ACS Appl. Mater. Interfaces. 1 (2009) 559-566. doi:10.1021/am800119q.

[15] E. Gustafsson, P.A. Larsson, L. Wågberg, Treatment of cellulose fibres with polyelectrolytes and wax colloids to create tailored highly hydrophobic fibrous networks, Colloids Surf. Physicochem. Eng. Aspects. 414 (2012) 415-421. doi:http://dx.doi.org/10.1016/j.colsurfa.2012.08.042.

[16] X. Rao, Y. Liu, Y. Fu, Y. Liu, H. Yu, Formation and properties of polyelectrolytes/TiO2 composite coating on wood surfaces through layer-by-layer assembly method, Holzforschung. 70 (2016) 361-367. doi:10.1515/hf-2015-0047.

[17] M.H. Freeman, D.D. Nicholas, T.P. Schultz, Nonarsenical wood protection: Alternative for chromated copper arsenate, creosote and pentachlorophenol. in: Timothy G. Townsend and Helena Solo-Gabriele (Eds.), Environmental Impacts of Treated Wood, CRCPress, Taylor and Francis Group, Boca Raton, FL 33487-2742, 2005, pp. 19-36.

[18] M.A. Lyth, Aqueous composition containing anionic polymer and wax emulsion, (1998).

[19] B. Lesar, M. Pavlič, M. Petrič, A.S. Škapin, M. Humar, Wax treatment of wood slows photodegradation, Polym. Degrad. Stab. 96 (2011) 1271-1278. doi:http://dx.doi.org/10.1016/j.polymdegradstab.2011.04.006.

[20] A. Lozhechnikova, K. Vahtikari, M. Hughes, M. Österberg, Toward energy efficiency through an optimized use of wood: The development of natural hydrophobic coatings that retain moisture-buffering ability, Energy Build. 105 (2015) 37-42. doi:http://dx.doi.org/10.1016/j.enbuild.2015.07.052.

[21] J. Milanovic, V. Manojlovic, S. Levic, N. Rajic, V. Nedovic, B. Bugarski, Microencapsulation of Flavors in Carnauba Wax, Sensors. 10 (2010). doi:10.3390/s100100901.

[22] L. Wang, S. Ando, Y. Ishida, H. Ohtani, S. Tsuge, T. Nakayama, Quantitative and discriminative analysis of carnauba waxes by reactive pyrolysis-GC in the presence of organic alkali using a vertical microfurnace pyrolyzer, J. Anal. Appl. Pyrolysis. 58–59 (2001) 525-537. doi:http://dx.doi.org/10.1016/S0165-2370(00)00155-8.

[23] T.H. Shellhammer, T.R. Rumsey, J.M. Krochta, Viscoelastic properties of edible lipids, J. Food Eng. 33 (1997) 305-320. doi:http://dx.doi.org/10.1016/S0260-8774(97)00030-7.

[24] S. Kheradmandnia, E. Vasheghani-Farahani, M. Nosrati, F. Atyabi, Preparation and characterization of ketoprofen-loaded solid lipid nanoparticles made from beeswax and carnauba wax, Nanomedicine: Nanotechnology, Biology and Medicine. 6 (2010) 753-759. doi:http://dx.doi.org/10.1016/j.nano.2010.06.003.

[25] J.R. Villalobos-Hernández, C.C. Müller-Goymann, Novel nanoparticulate carrier system based on carnauba wax and decyl oleate for the dispersion of inorganic sunscreens in aqueous media, European Journal of Pharmaceutics and Biopharmaceutics. 60 (2005) 113-122. doi:http://dx.doi.org/10.1016/j.ejpb.2004.11.002.

[26] A.R. Madureira, D.A. Campos, P. Fonte, S. Nunes, F. Reis, A.M. Gomes, B. Sarmento, M.M. Pintado, Characterization of solid lipid nanoparticles produced with carnauba wax for rosmarinic acid oral delivery, RSC Adv. 5 (2015) 22665-22673. doi:10.1039/c4ra15802d.

[27] I.S. Bayer, D. Fragouli, P.J. Martorana, L. Martiradonna, R. Cingolani, A. Athanassiou, Solvent resistant superhydrophobic films from self-emulsifying carnauba wax-alcohol emulsions, Soft Matter. 7 (2011) 7939-7943. doi:10.1039/c1sm05710c.

[28] F. Loosli, P. Le Coustumer, S. Stoll, TiO2 nanoparticles aggregation and disaggregation in presence of alginate and Suwannee River humic acids. pH and concentration effects on nanoparticle stability, Water Res. 47 (2013) 6052-6063. doi:http://dx.doi.org/10.1016/j.watres.2013.07.021.

[29] D. Harandi, H. Ahmadi, M. Mohammadi Achachluei, Comparison of TiO2 and ZnO nanoparticles for the improvement of consolidated wood with polyvinyl butyral against white rot, Int. Biodeterior. Biodegrad. 108 (2016) 142-148. doi:http://dx.doi.org/10.1016/j.ibiod.2015.12.017.

[30] E. Terzi, S.N. Kartal, N. Yılgör, L. Rautkari, T. Yoshimura, Role of various nano-particles in prevention of fungal decay, mold growth and termite attack in wood, and their effect on weathering properties and water repellency, Int. Biodeterior. Biodegrad. 107 (2016) 77-87. doi:http://dx.doi.org/10.1016/j.ibiod.2015.11.010.

[31] M.J. McGuffie, J. Hong, J.H. Bahng, E. Glynos, P.F. Green, N.A. Kotov, J.G. Younger, J.S. VanEpps, Zinc oxide nanoparticle suspensions and layer-by-layer coatings inhibit staphylococcal growth, Nanomedicine: Nanotechnology, Biology and Medicine. 12 (2016) 33-42. doi:http://dx.doi.org/10.1016/j.nano.2015.10.002.

505 [32] B. Pang, J. Yan, L. Yao, H. Liu, J. Guan, H. Wang, H. Liu, Preparation and characterization
506 of antibacterial paper coated with sodium lignosulfonate stabilized ZnO nanoparticles, RSC Adv.
507 6 (2016) 9753-9759. doi:10.1039/c5ra21434c.

508 [33] A. Degen, M. Kosec, Effect of pH and impurities on the surface charge of zinc oxide in
509 aqueous solution, J. Eur. Ceram. Soc. 20 (2000) 667-673. doi:10.1016/S0955-2219(99)00203-4.

510 [34] C. Rode, Moisture Buffering of Building Materials, Department of Civil Engineering,
511 Technical University of Denmark. BYG DTU R-126 (2005).

512 [35] K.K. Pandey, Study of the effect of photo-irradiation on the surface chemistry of wood,
513 Polym. Degrad. Stab. 90 (2005) 9-20.
514 doi:http://dx.doi.org/10.1016/j.polymdegradstab.2005.02.009.

515 [36] B. Ribeiro da Luz, Attenuated total reflectance spectroscopy of plant leaves: a tool for
516 ecological and botanical studies, New Phytol. 172 (2006) 305-318. doi:10.1111/j.1469-
517 8137.2006.01823.x.

518 [37] R.J. Hunter, Zeta Potential in Colloid Science : Principles and Applications, Academic
519 Press, London, 1981.

520 [38] P. Wagner, R. Fürstner, W. Barthlott, C. Neinhuis, Quantitative assessment to the structural
521 basis of water repellency in natural and technical surfaces, Journal of Experimental Botany. 54
522 (2003) 1295-1303. doi:10.1093/jxb/erg127.

523 [39] B. Michen, C. Geers, D. Vanhecke, C. Endes, B. Rothen-Rutishauser, S. Balog, A. Petri-
524 Fink, Avoiding drying-artifacts in transmission electron microscopy: Characterizing the size and
525 colloidal state of nanoparticles, Sci. Rep. 5 (2015). doi:10.1038/srep09793.

526 [40] U. Kallavus, K. Kärner, K. Kärner, M. Elomaa, Rapid semi-quantitative determination of
527 aspen lignin in lignocellulosic products, Proc. Est. Acad. Sci. 64 (2015) 105-112.
528 doi:10.3176/proc.2015.1S.06.

529 [41] B. George, E. Suttie, A. Merlin, X. Deglise, Photodegradation and photostabilisation of
530 wood - The state of the art, Polym Degradation Stab. 88 (2005) 268-274.
531 doi:10.1016/j.polymdegradstab.2004.10.018.

532 [42] X.-. Li, D. Reinhoudt, M. Crego-Calama, What do we need for a superhydrophobic surface?
533 A review on the recent progress in the preparation of superhydrophobic surfaces, Chem. Soc.
534 Rev. 36 (2007) 1350-1368.

535 [43] E. Celia, T. Darmanin, E. Taffin de Givenchy, S. Amigoni, F. Guittard, Recent advances in
536 designing superhydrophobic surfaces, J. Colloid Interface Sci. 402 (2013) 1-18.
537 doi:http://dx.doi.org/10.1016/j.jcis.2013.03.041.

[44] S. Wang, L. Jiang, Definition of superhydrophobic states, Adv Mater. 19 (2007) 3423-3424. doi:10.1002/adma.200700934.

[45] L. Feng, Y. Zhang, J. Xi, Y. Zhu, N. Wang, F. Xia, L. Jiang, Petal effect: A superhydrophobic state with high adhesive force, Langmuir. 24 (2008) 4114-4119. doi:10.1021/la703821h.

[46] C. Luo, M. Xiang, X. Liu, H. Wang, Transition from Cassie-Baxter to Wenzel States on microline-formed PDMS surfaces induced by evaporation or pressing of water droplets, Microfluid. Nanofluid. 10 (2011) 831-842. doi:10.1007/s10404-010-0714-0.

[47] H. Shaki, E. Vasheghani-Farahani, S.A. Shojaosadati, F. Ganji, Optimizing formulation variables of KCl loaded waxy microspheres, Iran. J. Pharm. Sci. 10 (2014) 37-54.

[48] M. Buchholz, P.G. Weidler, F. Bebensee, A. Nefedov, C. Wöll, Carbon dioxide adsorption on a ZnO(1010) substrate studied by infrared reflection absorption spectroscopy, Phys. Chem. Chem. Phys. 16 (2014) 1672-1678. doi:10.1039/c3cp54643h.

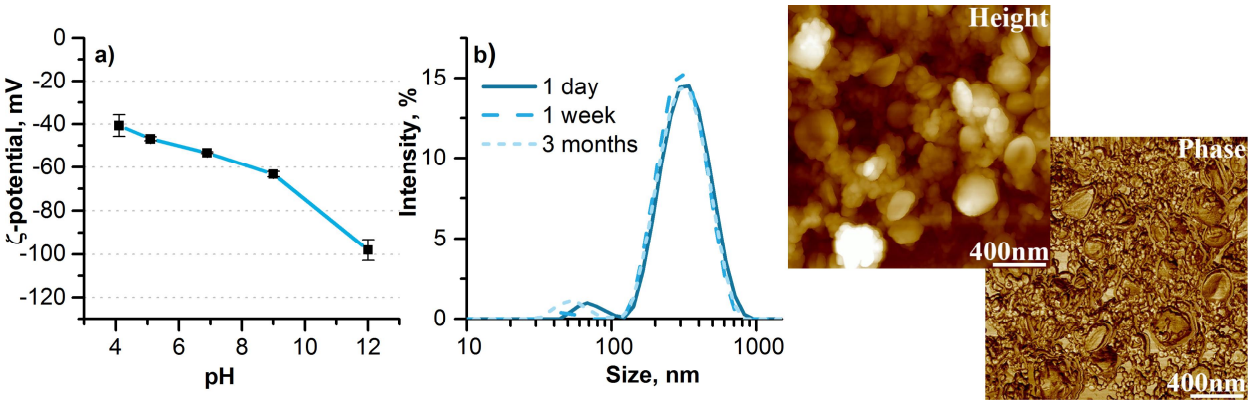


553

554 **Figure 1.** Influence of pH on the ζ-potential of wax particles (a) and particle size distribution
555 obtained from DLS measurements of the wax dispersion at pH 6.8-6.9 (b). AFM height (c) and
556 phase images (d) of wax dispersion dried on a freshly cleaved mica sheet. The wax dispersion was
557 prepared at a concentration of 1 g/L.

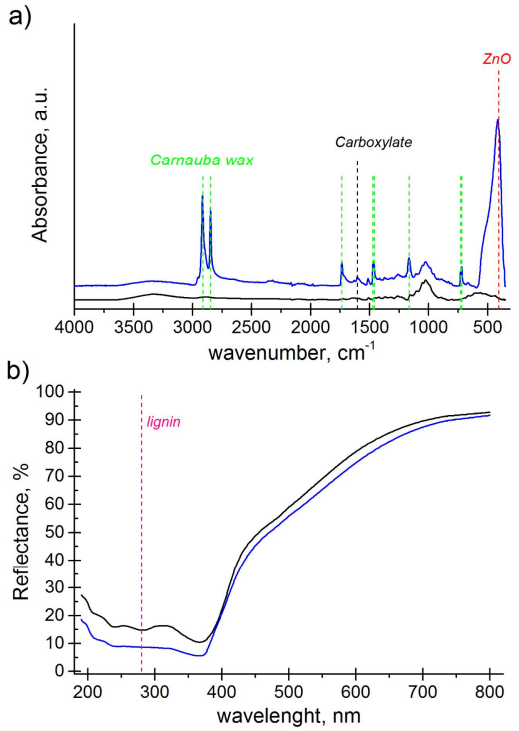


558

559 **Figure 2.** ATR-FTIR (a) and UV-Vis reflectance (b) spectra of uncoated spruce (black curves)
560 and spruce coated with 8 bilayers of ZnO/wax (blue curves). An inset (a) shows part of the spectra
561 at higher resolution.

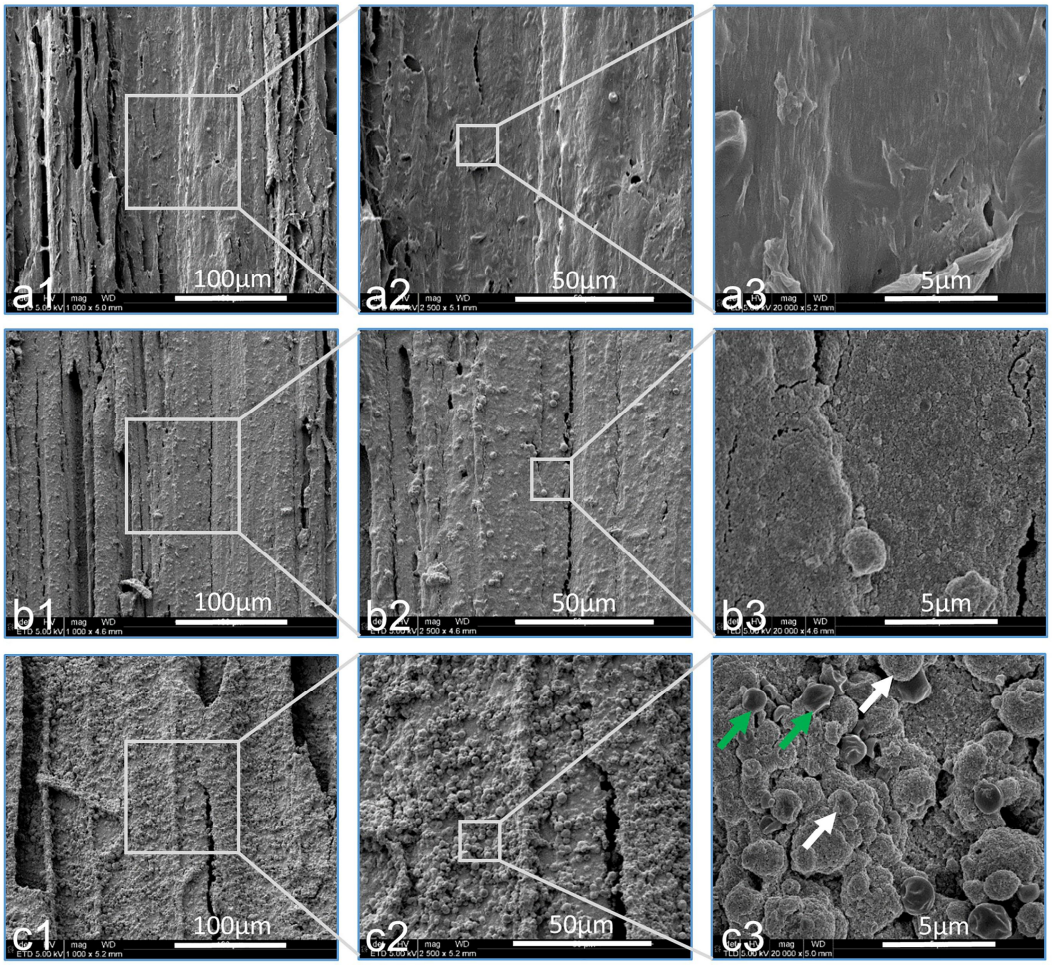


562

563 **Figure 3.** SEM images of unmodified wood (a) and wood coated with 8 bilayers of ZnO/wax at
564 wax concentration of 1 g/L (b) and 10 g/L (c).

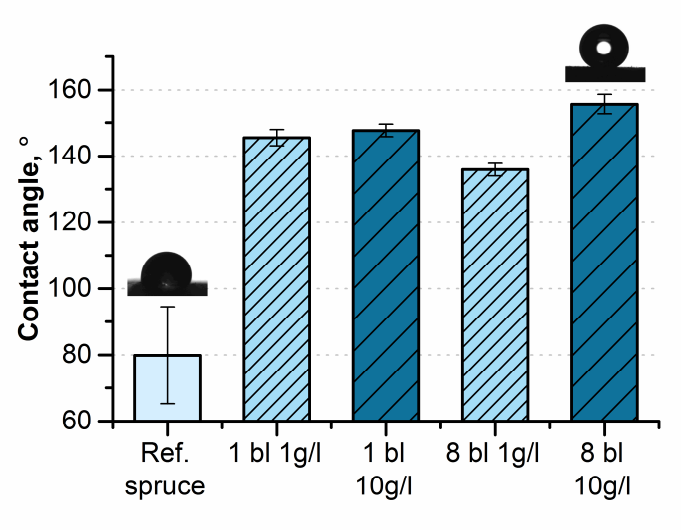


565

566 **Figure 4.** Contact angle of water measured after 1 minute on unmodified and differently coated
567 wood surfaces with 1 and 8 bilayers (bl) of ZnO and wax and with wax dispersion concentration
568 of 1 or 10 g/L.

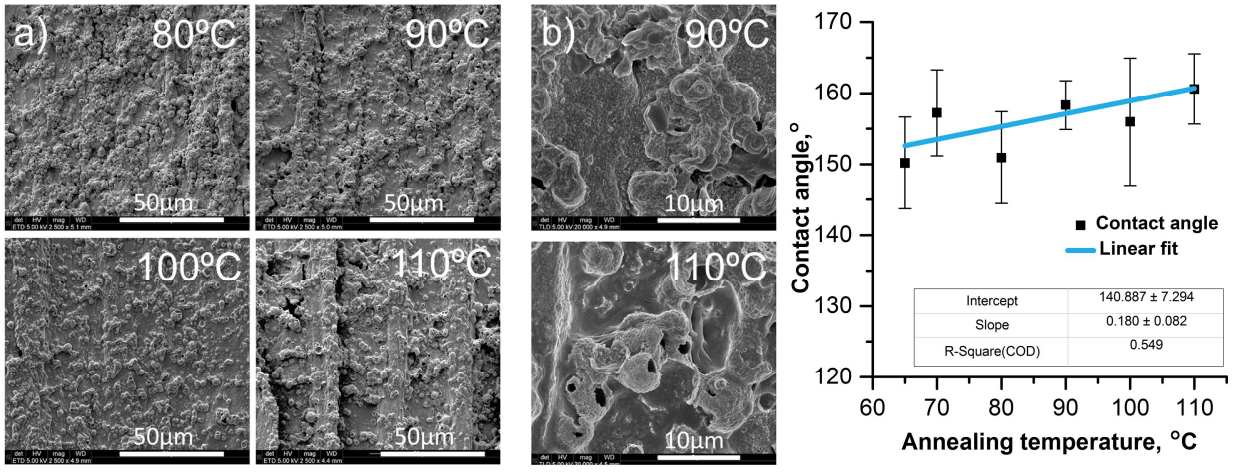


569

570 **Figure 5.** SEM images of thermally annealed coatings (8 bilayers, 10 g/L) at different
571 temperatures. (a) 2500× and (b) 20000× magnification. (c) Influence of thermal annealing
572 temperature on water CA on wood coated with 8 bilayers of 10 g/L ZnO/wax.

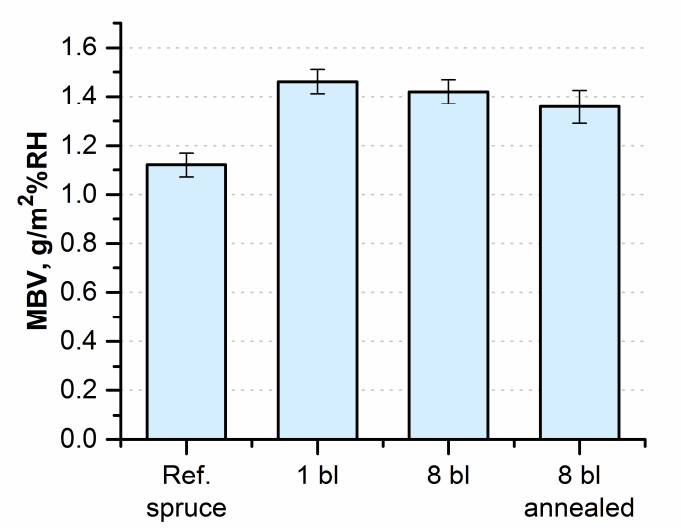


573

574 **Figure 6.** Influence of ZnO/wax coating (1 bilayer, 8 bilayers, and 8 bilayers annealed at 110ºC)

575 on MBV of wood. The dispersion concentrations of both ZnO and wax was 10 g/L.

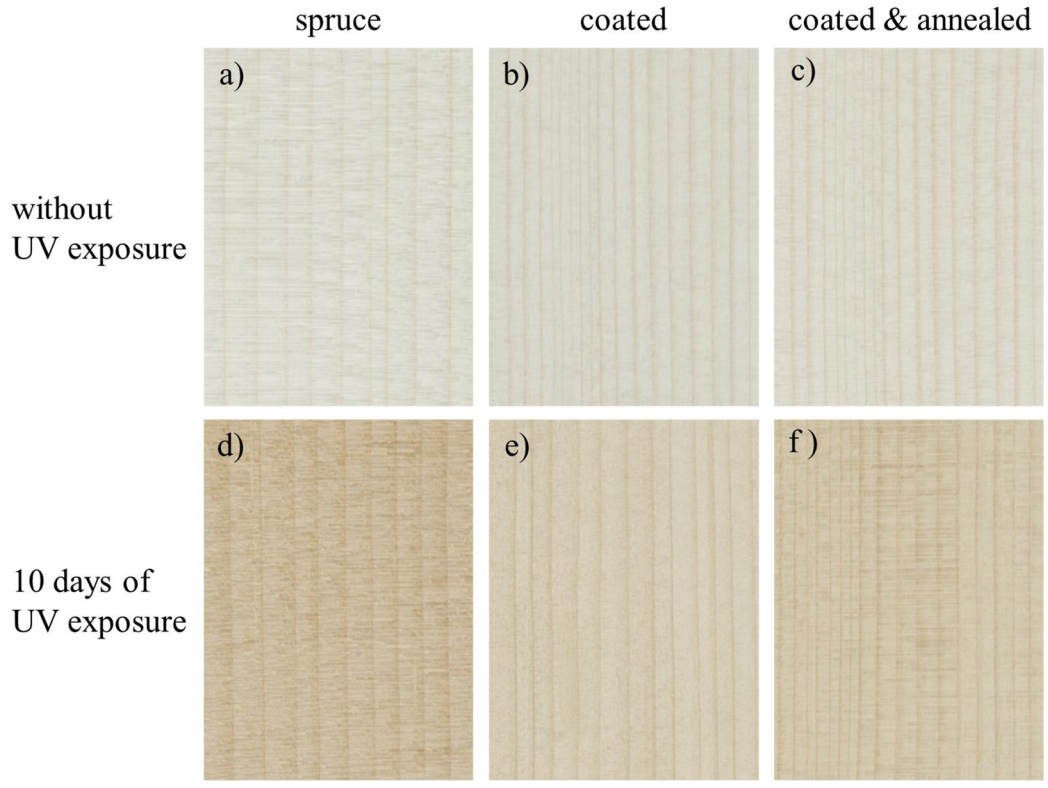


576

**Figure 7.** Photographs of original spruce (a), spruce coated with 8 bilayers ZnO/wax at 10 g/L without (b) and with annealing at 110°C (c). Spruce (d), spruce coated (e) as well as spruce coated and annealed (f) after UV exposure for 10 days. All photographs were taken with identical camera settings and illumination.

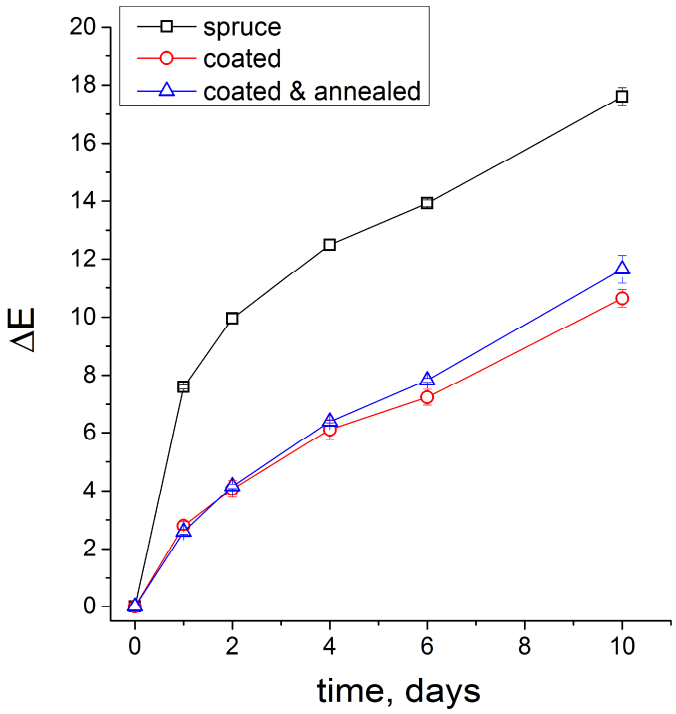


**Figure 8.** Total color change, ΔE, induced by UV exposure of uncoated spruce (black squares), spruce coated with 8 bilayers of ZnO/wax without (red circles) and with annealing at 110°C (blue triangles).

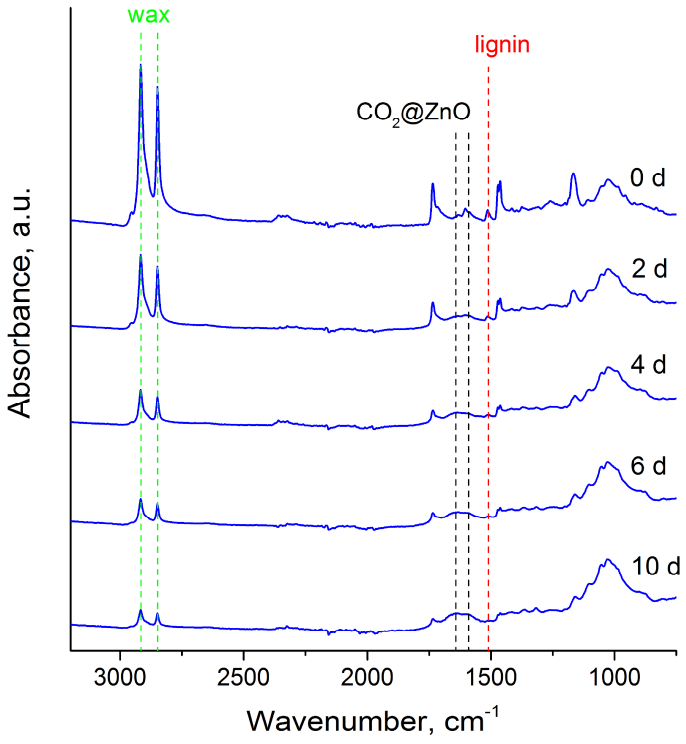


585

586 **Figure 9.** ATR-FTIR spectra of wood coated with 8 bilayers of 10g/L ZnO/wax after different

587 exposure time to UV light.

588